ЯДЕРНА ФІЗИКА ТА ЕНЕРГЕТИКА / NUCL. PHYS. AT. ENERGY 24 (2023) 209-218 ISSN 1818-331X

УДК 539.142+539.143 https://doi.org/10.15407/jnpae2023.03.209

Fahmi Sh. Radhi[1], Huda H. Kassim[2], Mushtaq A. Al-Jubbori[3], I. Hossain[4,*], Fadhil I. Sharrad[2,5], N. Aldahan[5], Hewa Y. Abdullah[6]

[1] *Department of Physics, College of Education for Pure Science, University of Basrah, Basrah, Iraq*
[2] *Department of Physics, College of Science, Karbala University, Karbala, Iraq*
[3] *Department of Physics, College of Education for Pure Sciences, University of Mosul, Mosul, Iraq*
[4] *Department of Physics, Rabigh College of Science & Arts, King Abdulaziz University, Rabigh, Saudi Arabia*
[5] *College of Health and Medical Technology, University of Alkafeel, Najaf, Iraq*
[6] *Physics Education Department, Faculty of Education, Tishk International University, Erbil, Iraq*

*Corresponding author: mihossain@kau.edu.sa

DESCRIPTION OF ENERGY LEVELS AND DECAY PROPERTIES IN ^{158}Gd NUCLEUS

In this paper, IBM-1 and IBM-2 with a SU(3) limit are used to describe the ^{158}Gd isotope. The calculations of energy levels in the ground state, beta-, and gamma-bands are made up, which account for 15 energy levels. However, we found that the energy states of the same spin of the beta- and vibrational bands become degenerate states. In breaking the SU(3) dynamical symmetry by introducing a value of pairing interaction, the degeneracy is lifted and the energy levels are brought up to the same order as the experimental ones.

Keywords: IBM-1, IBM-2, energy level, potential energy, ^{158}Gd.

1. Introduction

The ^{158}Gd nucleus has the main components of 64 protons and 94 neutrons, which are known as nucleons. The nuclear structure is complicated as each nucleon interacts with every other nucleon. Iachello and Arima [1] have successfully described the combined nuclear characters in intermediate-mass nuclei using the interacting boson model (IBM). Nevertheless, neutrons and protons did not differentiate in IBM-1. Depending on its angular momentum *L*, each boson can occupy one of two levels: the *s*-boson and the *d*-boson. The IBM-1 is established by a fixed number of bosons (N_b) for the low-lying combined state in even-even nuclei. Moreover, the IBM-1 model generated the algebraic U(6) group: O(6), SU(3), and U(5). These three dynamical symmetries are associated with gamma-soft, rotational, and vibrational nuclei, respectively [2, 3]. However, many researchers have suggested that nuclei have a transitional construction that consists of SU(3)-O(6), U(5)-O(6), and U(5)-SU(3) transitions [4, 5].

There are six stable isotopes $^{154-158,160}$Gd and one radioisotope ^{152}Gd. A great deal of research on the different kinds of bands and *B*(*E*2) strength in gadolinium isotopes with even mass (*A* = 152 - 156) was analyzed in Refs. [6 - 8]. Iachello and Zamfir [9] investigated quantum phase transitions in the microscopic structures of the Gd isotopes. The IBM-1 [10] delivers an amalgamated report of the joint nuclear conditions of Gd isotopes in terms of a system of interacting bosons. Lesher et al. [11] studied the ^{158}Gd (*n*, *n′*γ)-reaction with neutron energy up to 3.3 MeV to observe collective states of 0^+ and found two phonon γγ-strengths at 2276.7 keV. In another experiment, 13 excited 0^+ states below 3.1 MeV were observed in the ^{158}Gd nucleus by (*p*, *t*)-reactions [12]. Levon et al. [13] found collective properties of 0^+ levels in ^{158}Gd nuclei up to 4.2 MeV.

At present, we are choosing to study even-even ^{158}Gd isotopes because it has the greatest (0.25) usual abundance in Gd and belongs higher to the main shell *Z* = 50 and *N* = 82. This nucleus is currently assumed to have rotational-like properties. Recently, we have been studying IBM-1 calculations for rare earth nuclei with *N* = 100, 102, and 104 [14 - 16]. The basic IBM-1 results of the ^{158}Gd nucleus were presented by Zamfir et al. [17]. The structure of this nucleus was also studied in the ground state (g.s.) band up to 10^+, the gamma-band up to 6^+, and the beta-band up to 6^+ using the IBM spdf-model [18].

The aim of this article is to use IBM-1 and IBM-2 for calculating the different types of states for an even-even ^{158}Gd nucleus. At present, both models are applied for the ^{158}Gd nucleus, which is a deformed rotor. The scientific motivation for doing the present work is needed to compare the phenomenological interacting boson model, IBM-1, and its modification, IBM-2 to describe experimental data for the energies in the ^{158}Gd. In addition, the reduced transition probabilities *B*(*E*2) would be determined and compared to previously measured data. Also, both models are extended for the energy of g.s.-bands up to 12^+ levels. The main objective is to compare the three types of bands using IBM-1 and IBM-2 calculations to study the excited energy states and their decay properties. Moreover, the mixing ratios of 17 multipole transitions are calculated. These calculations have been reported for the first time.

2. Calculation procedure

2.1. IBM-1

For nuclei containing N nucleons, the IBM model assigns occupancy to a truncated model space. It is responsible for a numerical interpretation of indistinguishable particles with $L = 0$ or two forming pairs. In IBM-1, the Hamiltonian is written as [1, 19]:

$$H = \varepsilon_s \left(s^\dagger \cdot \tilde{s}\right) + \varepsilon_d \left(d^\dagger \cdot \tilde{d}\right) + \sum_{L=0,2,4} \frac{\sqrt{2L+1}}{2} C_L [[(d^\dagger \cdot d^\dagger]^{(L)} \cdot [\tilde{d} \cdot \tilde{d}]^{(L)}]^{(0)} +$$

$$+\frac{1}{\sqrt{2}}\upsilon_2\left[\left[d^\dagger \cdot d^\dagger\right]^{(2)} \cdot \left[\tilde{d}\cdot\tilde{s}\right]^{(2)} + \left[d^\dagger \cdot s^\dagger\right]^{(2)} \cdot [\tilde{d}\cdot\tilde{d}]^{(2)}\right]^{(0)} + \frac{1}{2}\upsilon_0\left[\left[d^\dagger \cdot d^\dagger\right]^{(0)} \cdot \left[\tilde{s}\cdot\tilde{s}\right]^{(0)} + \left[s^\dagger \cdot s^\dagger\right]^{(0)} \cdot [\tilde{d}\cdot\tilde{d}]^{(0)}\right]^{(0)} +$$

$$+\frac{1}{2}u_0\left[\left[s^\dagger \cdot s^\dagger\right]^{(0)} \cdot \left[\tilde{s}\cdot\tilde{s}\right]^{(0)}\right]^{(0)} + u_2\left[\left[d^\dagger \cdot s^\dagger\right]^{(2)} \cdot \left[\tilde{d}\cdot\tilde{s}\right]^{(2)}\right]^{(0)}. \quad (1)$$

The IBM-1 Hamiltonian can be described using nine terms, two of which appear in one-body terms (s and d), and ε_s and ε_d denote the energy of the boson, while the rest are two-body terms (C_0, C_1, C_4, $\upsilon_0, \upsilon_2, u_0, u_2$). The number of bosons N_b, on the other hand, is conserved. In general, the IBM-1 Hamiltonian in Eq. 1 is stated [20, 21]:

$$\hat{H} = \varepsilon\hat{n}_d + a_0\hat{P}\cdot\hat{P} + a_1\hat{L}\cdot\hat{L} + a_2\hat{Q}\cdot\hat{Q} + $$
$$+ a_3\hat{T}_3\cdot\hat{T}_3 + a_4\hat{T}_4\cdot\hat{T}_4, \quad (2)$$

Boson energy $\varepsilon = \varepsilon_d - \varepsilon_s$, and the operators are as follows:

$$\hat{n}_d = d^\dagger \cdot d, \qquad \hat{P} = 0.5\left[\left(\tilde{d}\cdot\tilde{d}\right) - \left(\tilde{s}\cdot\tilde{s}\right)\right],$$

$$\hat{L} = \sqrt{10}[d^\dagger \cdot \tilde{d}]^{(1)},$$

$$\hat{Q} = \left[d^\dagger\cdot\tilde{s} + s^\dagger\cdot\tilde{d}\right]^{(2)} + \chi\left[d^\dagger\cdot\tilde{d}\right]^{(2)},$$

$$\hat{T}_r = [d^\dagger \cdot \tilde{d}]^{(r)}. \quad (3)$$

The symbols $\hat{n}_d, \hat{P}, \hat{L}, \hat{Q}$ indicate the operator of the entire quantity of d-bosons, pairing, angular momentum, and quadrupole, respectively. The $\hat{T}_r$ operator represents octupole and hexadecapole as $r = 3$ and 4, respectively. The symbol χ refers to the quadrupole construction limits 0 and $\pm\frac{\sqrt{7}}{2}$ [22]. The strength parameters $a_0, a_1, a_2, a_3,$ and a_4 are used to describe the $\hat{P}, \hat{L}, \hat{Q}$, and $\hat{T}_r$ interactions between the bosons. The PHINT program's interaction parameters are specified: $\epsilon = EPS$, $a_0 = 2PAIR$, $a_1 = ELL/2$, and $a_3 = 5OCT$, $CHI = 0$.

The IBM-1 performs three types of dynamic symmetry: U(5), O(6), and SU(3), with their eigenvalues given by [21]

$$E\left(n_d,\upsilon,L\right) = \varepsilon n_d + \frac{a_1}{12}n_d\left(n_d+4\right) + \left(\frac{a_3}{7} - \frac{a_1}{10} - \frac{3a_4}{70}\right)\upsilon\left(\upsilon+3\right) + \frac{1}{14}\left(a_4 - a_3\right)L\left(L+1\right), \quad \text{U(5)}$$

$$E\left(\lambda,\mu,L\right) = \frac{a_2}{2}\left(\lambda^2+\mu^2+\lambda\mu+3\left(\lambda+\mu\right)\right) + \left(a_1 - \frac{2a_2}{8}\right)L\left(L+1\right), \quad \text{SU(3)}$$

$$E\left(\sigma,\tau,L\right) = \frac{a_0}{4}\left(N-\sigma\right)\left(N+\sigma+4\right) + \frac{a_3}{2}\tau\left(\tau+3\right) + \left(a_1 - \frac{a_3}{10}\right)\left(L\left(L+1\right)\right), \quad \text{O(6)} \quad (4)$$

Hence, the energy ϵ, pairing a_0, and quadrupole a_2 parameters correspond to the limits of U(5), O(6), and SU(3). Several nuclei have a property that allows them to transition between two or three of the above-mentioned limits.

The Hamiltonian [1, 19] is recognized for the calculations that break according to equations:

$$\hat{H} = a_0\hat{P}\cdot\hat{P} + a_1\hat{L}\cdot\hat{L} + a_2\hat{Q}\cdot\hat{Q}. \quad (5)$$

2.2. IBM-2

In the second type of IBM-2 [23, 24], it was accepted that the nuclei consist of neutrons and protons distinguished outside the major closed shells. Depending on its angular momentum *L*, each boson can occupy one of two levels: the *s*-boson and the *d*-boson. The practical formations in even proton- and even neutron-identical particles are paired to organize in states with $L = 0$ and $L = 2$. *S* indicates $L = 0$, and *d* indicates $L = 2$. The proton boson is indicated by π, and the neutron boson is indicated by ν. The s_π and s_ν indicate proton and neutron bosons with angular momentum $L = 0$. The symbols d_π and d_ν are the proton and neutron bosons with angular momentum $L = 2$.

The equation of Hamiltonian in IBM-2:

$$H = H_\nu + H_\pi + V_{\pi\nu}, \quad (6)$$

where H_ν and H_π are the neutron and proton boson Hamiltonians, while $V_{\pi\nu}$ is the proton-neutron interaction.

A simplified Hamiltonian [25]:

$$H = \varepsilon\left(\hat{n}_{d\pi} + \hat{n}_{d\nu}\right) + kQ_\pi \cdot Q_\nu + V_{\pi\pi} + V_{\nu\nu} + M_{\pi\nu}, \quad (7)$$

where $\varepsilon_\pi, \varepsilon_\nu$ are the proton and neutron energies, respectively, assumed equal $\left(\varepsilon_\pi = \varepsilon_\nu = \varepsilon\right)$, and the quadrupole operator is

$$Q_\rho = \left(d^\dagger \cdot s + s^\dagger \cdot \tilde{d}\right)^2_\rho + \chi_\rho\left(d^\dagger \cdot \tilde{d}\right)^2_\rho \qquad \rho = \pi, \nu, \quad (8)$$

where χ_ρ is a parameter to calculate the structure of the boson quadrupole operator.

The terms $V_{\pi\pi} + V_{\nu\nu}$ signify *d*-bosons conserving remaining proton-proton and neutron-neutron interactions. They are of the form

$$\hat{V}_{\rho\rho} = \sum_{k=1,2,4} \frac{1}{2}(2L+1)^{\frac{1}{2}} C_L^\rho \left[\left(d_\rho^\dagger \cdot d_\rho^\dagger\right)^{(L)} \cdot \left(\tilde{d}_\rho \cdot \tilde{d}_\rho\right)^{(L)}\right]^{(0)}. \quad (9)$$

The last term, $M_{\pi\nu}$, is the Majorana interactions, which have the form

$$M_{\pi\nu} = \xi_2\left(s_\nu^\dagger \cdot d_\pi^\dagger - d_\nu^\dagger \cdot s_\pi^\dagger\right)^2 . \left(s_\nu \cdot d_\pi^\dagger - d_\nu^\dagger \cdot s_\pi\right)^2 - -2\sum_{k=1,3}\xi_k\left(d_\nu^\dagger \cdot d_\pi^\dagger\right)^{(k)} \cdot \left(\tilde{d}_\nu \cdot \tilde{d}_\pi\right)^{(k)}. \quad (10)$$

If there is experimental evidence for mixed symmetry states, then the Majorana parameters are varied to fix the location of these states in the spectrum.

For energy level calculations, the computer code NPBOS [26] is used to diagonalize the Hamiltonian (Eq. 7) and allow the parameters ε, k, x_π, x_ν and C_L to vary until one obtains the best fit for the experimental data.

3. Outcomes and discussion

3.1. Energy levels in ^{158}Gd

The paper seeks to explain the excitation spectra and other properties of the nucleus ^{158}Gd using the SU(3) limits of IBM-1 and IBM-2. We have calculated energy levels using IBM-1 and IBM-2 models, as well as electromagnetic transition probabilities and potential energy surface (PES) levels using IBM-1 and IBM-2 models. The energy levels, the strength of *B*(*E*2), the level energy ratios, and the PES for ^{158}Gd are discussed comprehensively.

The straightforward method for determining the IBM-1 parameters is to use the energy ratio (*R*) as a starting point for calculations. The energy ratio, $R = E4_1^+ / E2_1^+$, indicates the symmetry form of a nucleus. The patterns $E4_1^+$ and $E2_1^+$ correspond to the energy levels 4_1^+ (261 keV) and 2_1^+ (79.5 keV), respectively. It is well understood that $R \approx 3.33$ is for deformed nuclei SU(3), $R \approx 2.50$ is for gamma-unstable nuclei or O(6), and $R \approx 2$ is for vibrational nuclei U(5) [27 - 29]. The energy ratio $R = E4_1^+ / E2_1^+$ for this nucleus is 3.30 indicating a deformed nucleus SU(3).

The following Tables give information on all energy states, band structure, *E*2-transitions, mixing ratios, and individual states that contain the final results of ^{158}Gd.

The best values for the limits that provide a suitable fit between the theoretical IBM-1 and measured levels of the ^{158}Gd are given in Table 1, while Table 2 displays the best-fitting data for the calculation of IBM-2.

Table 1. **The parameters in the IBM-1 calculation for ^{158}Gd**

Nucleus	N_b	a_0	a_1	a_2	χ
^{158}Gd	13	0.00328	0.0135	–0.0300	–1.33

Table 2. **The parameters in the IBM-2 calculation for ^{158}Gd**

A	N_π	N_υ	*k*	χ_ν	χ_π	ED	C_ν^0	C_π^2
^{158}Gd	7	6	–0.078	–0.850	–0.925	0.360	0.050	0.050

The results of the energy levels of experiments [18, 27 - 29] and calculations by both models of the ^{158}Gd isotope are presented in Table 3. The physical criterion of the quality of agreement between the experimental states and the calculated results is presented as a percentage of error as shown in this Table, the IBM-1 and IBM-2 computations are settled fairly with the available investigational results.

Table 3. **The energy levels of the ^{158}Gd nucleus by IBM-1 and IBM-2 calculations**

Experiment		IBM				
		IBM-2		Error	IBM-1	Error
J^+	keV	J_i^+	keV	%	keV	%
2	80	2_1	83	3.8	74	8.5
4	261	4_1	260	0.38	246	5.7
6	539	6_1	547	1.48	516	4.3
8	904	8_1	930	2.88	884	2.2
2	1187	2_2	1133	4.55	1194	0.6
0	1196	0_2	1281	7.11	1196	0
2	1260	2_3	1273	1.03	1270	0.8
3	1266	3_1	1265	0.08	1268	0.16
10	1350	10_1	1442	6.81	1352	0.15
4	1358	4_2	1351	0.52	1366	0.59
4	1381	4_3	1369	0.87		
4	1407	4_4	1672	18.8	2308	64.0
0	1452	0_3	1472	1.8		
5	1481	5_1	1513	2.2	1489	0.54
5	1499	5_2	1588	0.9		
2	1517	2_4	1427	6.3		
6	1624	6_2	1589	2.2	1636	0.74
6	1636	6_3	1701	3.9	1712	4.65
(4)	1667	4_5	1747	4.8		
0	1743	0_4	2038	16.6		
2	1792	2_5	1516	15.4		
1	1848	1_1	1276	30.9		
12	1865	12_1	2059	10.4	1917	2.78
(2)	1895	2_6	1613	14.9		
4	1902	4_6	1892	0.5		
4	1920	4_7	2116	10.2		
1	1930	1_2	2299	19.12		
3	1941	3_2	1381	28.85		
0	1957	0_5	2337	19.4		
2	1964	2_7	2106	7.2		
(5	2018	5_3	1919	4.9		
$1^+, 2^+$	2355	1_3	2417	2.6		
3	2034	3_3	1628	19.9		
(2)	2036	2_8	2307	13.3		
2	2084	2_9	2341	12.3		
(4)	2095	4_8	2357	12.5		
2^+, 3	2276	2_{10}	2412	5.9		
0	2277	0_6	2477	8.8		
0	2340	0_7	2545	8.5		
2	2340	2_{11}	2466	5.4		
$1^{(+)}$	2565	1_4	2538	1.0		
(3)	2395	3_4	2302	3.9		
1, 2^+	2451	2_{12}	2502	2.1		
(2)	2539	2_{13}	2520	0.7		
(3)	2600	3_5	2362	9.1		
$1^{(+)}$	2600.3	1_5	2681	3.1		
0	2644	0_8	2611	1.2		
1, 2^+	2674	2_{14}	2646	1.1		

Continuation of Table 3

Experiment		IBM				
		IBM-2		Error	IBM-1	Error
J^+	keV		keV	%	keV	%
$1^{(+)}$	2686	1_6	2764	2.8		
0	2687	0_9	2825	5.1		
2^+, 3	2701	2_{15}	2712	0.4		
1, 2^+	2805	2_{16}	2749	2.0		
2^+, 3	2879	2_{17}	2852	0.9		
0	2910	0_{10}	2865	1.5		
2	2964	J_i^+ 2_{18}	2923	1.4		
$1^{(+)}$	2986	1_7	3212	7.6		
2^+, 3	3060	2_{19}	2990	2.3		
0	3077	0_{11}	2941	4.4		
0	3110	0_{12}	3321	6.8		
1	3192	1_8	3285	2.9		
2^+, 3	3201	2_{20}	3127	2.3		
1	3202	1_9	3371	5.3		
		1_{10}	3577			

3.2. Comparative studies of the g.s.-, gamma-, and beta-bands

The comparative study with the g.s.-, beta-, and gamma-bands in the present work of IBM-1 and IBM-2 is compared with previous spdf-IBM data [18] and measured data [18, 28 - 30] as shown in Table 4. The g.s.-band of the present works is raised from 10^+ (1349.5 keV) [18] to 12^+ (1865 keV) in the ^{158}Ge nucleus. The average error of the previous spdf-IBM data for the g.s.-band was 13.98 % [18], where as the corresponding present work for IBM-1 and IBM-2 is 3.78 and 4.28 %, respectively. The average percentage of deviation for the gamma-band is 0.48 [18], and the corresponding values for IBM-1 and IBM-2 are 0.52 and 1.8 %, respectively. The present calculated data for both models for the beta-band from 0^+ to 6^+ are consistent with Ref. [18], except for 4^+ levels. Neglecting the calculated 4^+ level the average values of errors are 1.81, 4.03, and 3.54 % for the calculated IBM-1, IBM-2, and reference values, respectively. Therefore, the present calculations are more reliable than those of previous calculations [18] and the performance of IBM-1 is better than IBM-2 for even-even ^{158}Gd nuclei.

Table 4. **Comparative study of energy levels of the g.s.-band, gamma-band, and beta-band of ^{158}Gd in previous experiment, spdf-IBM [18] and present work of IBM-1 and IBM-2**

Type	J^+	Experiment [18], keV	spdf-IBM [18], keV	Δ_1 [18], %	Present IBM-1, keV	Δ_2, %	Present IBM-2, keV	Δ_3, %
g.s.-band	2^+	80	67	16.25	74	7,50	83	3.75
	4^+	261	223	14.56	246	5.75	260	0.38
	6^+	539	463	14.10	516	4.27	547	1.48
	8^+	904	786	13.05	884	2.21	930	2.88
	10^+	1350	1189	11.93	1352	0.15	1442	6.81
	12^+	1865	–	–	1917	2.79	2059	10.40
gamma-band	2^+	1187	1186	0.08	1194	0.59	1133	4.55
	3^+	1266	1270	0.32	1268	0.16	1265	0.08
	4^+	1358	1361	0.22	1366	0.59	1351	0.52
	5^+	1481	1504	1.55	1489	0.54	1513	2.16
	6^+	1624	1620	0.25	1636	0.74	1589	2.16
beta-band	0^+	1196	1168	2.34	1196	0.00	1281	7.11
	2^+	1260	1258	0.16	1270	0.79	1273	1.03
	4^+	1407	1461	3.77	2308	64	1672	18.83
	6^+	1636	1765	7.89	1712	4.65	1701	3.97

N o t e. The percentage of deviation Δ_1, Δ_2, and Δ_3 calculated from Ref. 18, present work of IBM-1 and IBM-2, respectively.

It is found that the energy states of the 0_2^+ beta- and 2_1^+ vibrational bands show degenerate states. The degeneracy in the beta- and gamma-bands uses a more generalized Hamiltonian to get rid of that. The degeneracy is well known in the SU(3) limit of the Hamiltonian. In breaking the SU(3) dynamical symmetry by introducing a value of pairing interaction, the degeneracy is lifted, and the energy levels are brought up to the right order as the experimental ones.

3.3. *B*(*E*2) in IBM-1

The *B*(*E*2) strength of ^{158}Gd in IBM-1 [1, 19, 30] is calculated:

$$T^{E2} = \alpha_2\left[d^\dagger \cdot s + s^\dagger \cdot d\right]^{(2)} + \beta_2\left[d^\dagger \cdot d\right]^{(2)} = e_B\hat{Q}. \tag{11}$$

The symbol ($s^\dagger$, $d^\dagger$) is the creation and (s, d) is the annihilation operators for *s*- and *d*-bosons, respectively, although α_2 and β_2 symbols are two parameters. α_2 = e_B effective charge of boson and $\beta_2 = \chi\alpha_2$.

The *B*(*E*2) value for the SU(3) limits [19]:

$$\text{SU(3)}: \; B\left(E2; L \to L-2\right) =$$

$$= {e_B}^2 \frac{3(L+2)(L+1)}{4(2L+3)(2L+5)}(2N-L)(2N+L+3). \tag{12}$$

The effective charge is calculated from the measured data [28], $B\left(E2; 2_1^+ \to 0_1^+\right)$, presented in Table 5.

Table 5. **Parameters (in eb) to reproduce *B*(*E*2) values for ^{158}Gd using IBM-1**

A	N_b	α_2	β_2
^{158}Gd	13	0.145	–0.185

3.4. *B*(*E*2) in IBM-2

The model wave functions were found by diagonalization of the IBM-2 Hamiltonian, and the program NPBEM [27] was used to estimate the electromagnetic transition. The *E*2-transition operator [31]:

$$T^{(E2)} = e_\pi Q_\pi + e_\nu Q_\nu, \tag{13}$$

where Q_ρ is the quadrupole operator and has the same definition as in Hamiltonian (7). e_π and e_ν are boson effective charges depending on the boson number *N*, and they can be obtained by fitting $B\left(E2: 2_1^+ \to 0_1^+\right)$ to the experimental data (Table 6). The comparison between the IBM-1 and IBM-2 calculations of *B*(*E*2) values in ^{158}Gd is presented in Table 7.

Table 6. **Parameters (in eb) to reproduce *B*(*E*2) values for even-even ^{158}Gd isotope using IBM-2**

A	N_π	N_υ	e_π	e_ν
^{158}Gd	7	6	0.180	0.100

Table 7. **The *B*(*E*2) values in ^{158}Gd nucleus**

Experimental *B*(*E*2) (e^2b^2) values in ^{158}Gd compared with IBM predictions						
E_i	J_i^+K	E_f	J_f^+K	Experiment [25, 26]	IBM	
					IBM-1	IBM-2
g.s.-band						
80	2 0_1	0.00	0 0_1	1.01(3)	1.0683	1.0578
261	4 0_1	80	2 0_1	1.47(3)	1.5057	1.4953
539	6 0_1	261	4 0_1	–	1.6179	1.5996
904	8 0_1	539	6 0_1	1.68(2)	1.6325	1.5967
g.s.-band						
1350	10 0_1	904	8 0_1	1.73(2)	1.5948	1.5229
1865	12 0_1	1350	10 0_1	1.58(2)	1.5200	1.3793
Q_{2_1}				−2.01(4)	–2.0894	–2.0817
gamma-band						
1358	4 2_1	1187	2 2_1	$0.58\binom{85}{7}$	0.5210	0.4365
beta-band → g.s.-band						
1196	0 0_2	80	2 0_1	$0.0059\binom{213}{7}$	0.0092	0.0274
1260	2 0_2	0.00	0 0_1	0.0016(2)	0.0015	0.0070
	2 0_2	80	2 0_1	0.00040(7)	0.0024	0.0039
	2 0_2	261	4 0_1	0.0071(8)	0.0054	0.0005

Continuation of Table 7

Experimental $B(E2)$ (e^2b^2) values in ^{158}Gd compared with IBM predictions						
E_i	J_i^+K	E_f	J_f^+K	Experiment [25, 26]	IBM	
					IBM-1	IBM-2
1407	$4\ 0_2$	80	$2\ 0_1$	$0.0067\binom{134}{10}$	0.0017	0.0011
		261	$4\ 0_1$	$0.0018\binom{37}{3}$	0.0021	0.0007
		539	$6\ 0_1$	$0.0158\binom{316}{23}$	0.0053	0.0100
1920	$1\ 1_2$	1187	$2\ 2_1$	–		0.0037
gamma-vibrational band → g.s.-band						
1187	$2\ 2_1$	0.00	$0\ 0_1$	0.017(2)	0.0130	0.0387
	$2\ 2_1$	80	$2\ 0_1$	0.031(4)	0.0204	0.0387
	$2\ 2_1$	261	$4\ 0_1$	0.0014(2)	0.0013	0.0054
1266	$3\ 2_1$	80	$2\ 0_1$	$0.0178\binom{329}{17}$	0.0228	0.0428
		261	$4\ 0_1$	$0.010\binom{17}{1}$	0.0116	0.0281
1358	$4\ 2_1$	80	$2\ 0_1$	$0.0057\binom{84}{7}$	0.0067	0.0065
		261	$4\ 0_1$	$0.037\binom{54}{5}$	0.0240	0.0506
		539	$6\ 0_1$	> 0.0048	0.0033	0.0017
$K = 4_1$ band → g.s.-band						
1381	$4\ 4_1$	261	$4\ 0_1$	–		0.0109
1499	$5\ 4_1$	261	$4\ 0_1$	–		0.0005
$K = 0_3$ band → g.s.-band						
1452	$0\ 0_3$	80	$2\ 0_1$	$0.0107\binom{683}{15}$		0.0010
1517	$2\ 0_3$	0.00	$0\ 0_1$	0.00188(25)		0.0014
		80	$2\ 0_1$	–		0.0017
		261	$4\ 0_1$	0.00193(31)		0.0188
$K = 0_3$ band → gamma-vibrational band						
1517	$2\ 0_3$	1358	$4\ 2_1$	0.1224(408)		0.0685
$K = 0_4$ band → g.s.-band						
1743	$0\ 0_4$	80	$2\ 0_1$	< 0.00459		0.0009

3.5. Mixing ratios

The $M1$ transition operator can be written as

$$T^{(M1)} = \sqrt{3/4\pi}(g_\pi L_\pi + g_\nu L_\nu). \qquad (14)$$

The L_ρ operators are the angular momentum operators for the proton and neutron and are defined to be $L_\rho = \sqrt{10}\left(\tilde{d}_\rho d_\rho^\dagger\right)^{(1)}$.

g_π and (g_ν) are the proton (neutron) boson g-factors. Their values are determined by fitting to the experimental value of the g-factor of the 2_1^+ state $(g_{2_1^+})$.

Having obtained the values of the reduced $E2$ and $M1$ matrix elements, one can proceed to calculate multipole mixing ratios (δ). They are defined [31, 32] as

$$\delta\left(\frac{E2}{M1}\right) = 0.835 E_\gamma\left(\text{MeV}\right)\cdot\Delta, \qquad (15)$$

where Δ is the ratio of the reduced $E2$ matrix elements to the reduced $M1$ matrix elements and determines the sign of δ. E_γ is the energy of gamma-ray transition. The boson g-factor for neutrons and protons is given in Table 8. The mixing ratios (δ) in IBM-2 are presented in Table 9.

Table 8. **The boson g-factors used in the calculations**

A	N_π	$N\upsilon$	g_ν	g_π
^{158}Gd	7	6	0.34	0.44

Also, with these boson g-factors, the IBM-2 calculation gives g_{2_1} a value of +0.39, which is in perfect agreement with experiment +0.387(4).

Table 9. **Comparison of mixing ratio in measured data [27, 33] and IBM-2**

IBM-2 mixing ratios (δ) in comparison with available experimental [27, 33] data in ^{158}Gd						
E_i (level), keV	J_i^+K	E_f (level), keV	J_f^+K	E_γ, keV	δ(*e*, *b*/μ_N) Experiment	δ(*e*, *b*/μ_N) IBM-2
1187	2 2_1	80	2 0_1	1107.63	+ 80 < δ < –25, – 9.0(15)*	+87.82
1260	2 0_2	80	2 0_1	1180	–0.70(7)	–0.68
1266	3 2_1	80	2 0_1	1186	$+30\left(^{32}_{14}\right)$	+23.56
	3 2_1	261	4 0_1	1004	$-23\left(^{19}_{7}\right)$	+15.51
1358	4 2_1	261	4 0_1	1097	$+6.4\left(^{14}_{10}\right)$, –0.73(4)	+6.4
1380	4 4_1	261	4 0_1	1119	$-4.5\left(^{20}_{17}\right)$	–1.02
1407	4 0_2	261	4 0_1	1145	+1.0(2)	+1.20
1499	5 4_1	261	4 0_1	1237	>1*	+.50
1517	2 0_3	80	2 0_1	1437.89	−1.5(4)	+1.23
1667	4 0_3	261	4 0_1	1405.84	+6(2), –0.76(11)	+0.39
1920	4 4_2	1380.69	4 4_1	539	−0.02(9), +1.08(17).	+12.38
1930	1 1_2	1187	2 2_1	743.08	+0.17(15)	+0.43
1964	2 1_2	80	2 0_1 0_1	1884.64	−0.08(12), $+2.9\left(^{18}_{9}\right)$	–251.48
2036	(2)	80	2 0_1	1955.76	+0.06(6), +2.0(3)	+0.0011
2089	2	80	2 0_1	2009.9	+0.45(20), $+7\left(^{70}_{4}\right)$	+0.14
		1187.14	2 2_1	902.07	+1.5(7)	–0.20
2095	(4)	261	4 0_1	1833.73	−0.25(13), +1.8(6)	–19.52

3.6. PES

The PES application provides information for determining the microscopic and geometric shapes of nuclei. IBM Hamiltonian [33 - 36] produced the PES plots using the Skyrme mean field procedure. The IBM-1 energy surface is created by combining the IBM-1 Hamiltonian’s expectation value (Eq. 1) with the coherent state ($|N,\beta,\gamma\rangle$ [19]. The creation operators (b_c^+) act on a state of boson vacuum $|0\rangle$ to produce the coherent state as follows:

$$|N,\beta,\gamma = \frac{1}{\sqrt{N!}}\,(b_c^\dagger)^N\ |0\rangle, \tag{16}$$

where

$$b_c^\dagger = \frac{1}{\sqrt{1+\beta^2}}\left\{s^\dagger + \beta\left[cos\gamma\left(d_o^\dagger\right) + \sqrt{1/2}\,sin\gamma\left(d_2^\dagger + d_{-2}^\dagger\right)\right]\right\}, \tag{17}$$

then, the PES can be written in terms of β and γ as

$$E\left(N,\beta,\gamma\right) = \frac{N\varepsilon_d\beta^2}{\left(1+\beta^2\right)} + \frac{N\left(N+1\right)}{(1+\beta^2)^2}\left[\alpha_1\beta^4 + \alpha_2\beta^3 cos3\gamma + \alpha_3\beta^2 + \alpha_4\right], \tag{18}$$

where α parameters are associated with the coefficient of C_L, v_2, v_o, and u_o, as seen in Eq. (1). The term β refers to a nucleus’s total deformation. Then, the shape of a nucleus could be spherical or distorted depending on whether β = 0 or not. Moreover, the variation in nucleus symmetry is represented by gamma-term, when γ = 0, the nucleus has a prolate shape; when γ = 60, it has an oblate shape. As it is seen from Figure the nucleus has prolate shape.

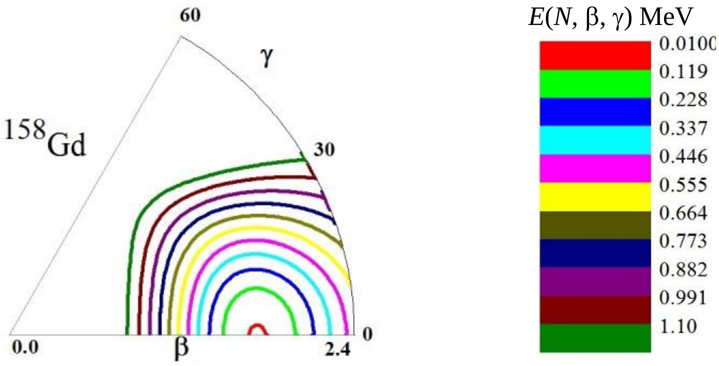

The PES contour plot for ^{158}Gd nuclei. The color panel represents the PES values in MeV.
(See color Figure on the journal website.)

4. Conclusions

The ground energy and other states, electromagnetic transition, and PES of the ^{158}Gd nucleus were all theoretically calculated using the IBM-1 and IBM-2 methods. The results of the ground and other energy levels of this nucleus are consistent with previous experimental data. The calculation of the present work of the g.s.-, gamma-, and beta-bands is better than the previously calculated reference [18]. Furthermore, the reduced transition probabilities $B(E2)$ results of IBM-1 calculations are coherent with the available experimental data. The energy states of the beta- and vibrational bands show degenerate states. The ^{158}Gd nucleus under discussion has a limit of SU(3). In breaking the SU(3) dynamical symmetry by introducing a value of pairing interaction, the degeneracy is lifted and the energy levels are brought up to the right order as the experimental ones.

We are grateful to the University of Mosul, the College of Education for Pure Sciences, Department of Physics for their assistance with this research work.

REFERENCES

1. F. Iachello, A. Arima. *The Interacting Boson Model* (Cambridge, Cambridge University Press, 1987).
2. G.L. Long, S.J. Zhu, H.Z. Sun. Description of ^{116,118,120}Cd in the interacting boson model. J. Phys. G: Nucl. Part. Phys. 21 (1995) 331.
3. F. Iachello. Analytic Description of Critical Point Nuclei in a Spherical-Axially Deformed Shape Phase Transition. Phys. Rev. Lett. 87 (2001) 525052.
4. P. Cejnar, J. Jolie, R.F. Casten. Quantum phase transitions in the shapes of atomic nuclei. Rev. Mod. Phys. 82 (2010) 2155.
5. R.F. Casten, E.A. McCutchan. Quantum phase transitions and structural evolution in nuclei. J. Phys. G: Nucl. Part. Phys. 34 (2007) R285.
6. H.R. Yazar et al. The Investigation of Electromagnetic Transition Probabilities of Gadolinium Isotopes with the IBFM-1 Model. Chin. J. Phys. 48(3) (2010) 344.
7. J.E. García-Ramos et al. Two-neutron separation energies, binding energies and phase transitions in the interacting boson model. Nucl. Physics A 688 (2001) 735.
8. J.E. García-Ramos et al. Phase transitions and critical points in the rare-earth region. Phys. Rev. C 68 (2003) 024307.
9. F. Iachello, N.V. Zamfir. Quantum Phase Transitions in Mesoscopic Systems. Phys. Rev. Lett. 92 (2004) 212501.
10. M.J.A. de Voigt, J. Dudek, Z. Szymański. High-spin phenomena in atomic nuclei. Rev. Mod. Phys. 55 (1983) 949.
11. S.R. Lesher et al. New 0^+ states in ^{158}Gd. Phys. Rev C 66 (2002) 051305.
12. S.R. Lesher et al. Study of 0^+ excitations in ^{158}Gd with the (n, n′γ) reaction. Phys. Rev. C 76 (2007) 034318.
13. A.I. Levon et al. New data on 0^+ states in ^{158}Gd. Phys. Rev. C 100 (2019) 034307.
14. M.A. Al-Jubbori et al. Deformation properties of the even-even rare-earth Er-Os isotopes for N = 100. Int. J. Mod. Phys. E 27 (2018) 1850035.
15. M.A. Al-Jubbori et al. Nuclear structure of the even-even rare-earth Er-Os nuclei for N = 102. Indian J. Phys. 94(3) (2020) 379.
16. M.A. Al-Jubbori et al. Nuclear Structure of Rare-Earth ^{172}Er, ^{174}Yb, ^{176}Hf, ^{178}W, ^{180}Os Nuclei. Ukr. J. Phys. 67(2) (2022) 127.
17. N.V. Zamfir, Jing-ye Zhang, R.F. Casten. Interpreting recent measurements of 0^+ states in ^{158}Gd. Phys. Rev. C 66 (2002) 057303.
18. A.I. Levon et al. High-resolution study of excited states in ^{158}Gd with the (p, t) reaction. Phys. Rev. C 102 (2020) 014308.
19. R.F. Casten, D.D. Warner. The interacting boson approximation. Rev. Mod. Phys. 60 (1988) 389.
20. A. Arima, F. Iachello. Interacting boson model of collective nuclear states II. The rotational limit. Ann. Phys. 111 (1978) 201.
21. A. Arima, F. Iachello. Interacting boson model of

collective states I. The vibrational limit. Ann. Phys. 99 (1976) 253.
22. F. Iachello. Dynamical Supersymmetries in Nuclei. Phys. Rev. Lett. 44 (1980) 772.
23. A. Arima et al. Collective nuclear states as symmetric couplings of proton and neutron excitations. Phys. Lett. B 66(3) (1977) 205.
24. T. Otsuka et al. Shell model description of interacting bosons. Phys. Lett. B 76 (1978) 139.
25. G. Puddu, O. Scholten, T. Otsuka. Collective Quadrupole States of Xe, Ba and Ce in the Interacting Boson Model. Nucl. Phys. A 348 (1980) 109.
26. T. Otsuka, N. Yoshida. User's manual of the program NPBOS. Report JAERI-M 85-094 (Japan Atomic Energy Research Institute, 1985) 57 p.
27. http://www.nndc.bnl.gov/ensdf/DatasetFetchServlet
28. R.G. Helmer. Nuclear Data Sheets for A = 158. Nuclear Data Sheets 101 (2004) 325.
29. N. Nica. Nuclear Data Sheets for A = 158. Nucl. Data Sheets 141 (2017) 1.
30. H.H. Kassim. Description of the Ba - Dy (N = 92) nuclei in the interacting boson model. Int. J. Mod. Phys. E 26(4) (2017) 1750019.
31. O. Scholten, A.E.L. Dieperink. In: *Interacting Boson-Fermi Systems in Nuclei*. Proc. of a seminar, Erice, Italy, June 1980. F. Iachello (Ed.) (New York, Plenum, 1981).
32. J. Lange, K. Kumar, J.H. Hamilton. E0-E2-M1 multipole admixtures of transitions in even-even nuclei. Rev. Mod. Phys. 54 (1982) 119.
33. L.I. Govor, A.M. Demidov, I.V. Mikhailov. Multipole mixtures in gamma transitions in ^{158}Gd from the (n, n′γ) reaction. Phys. of Atom. Nuclei 64 (2001) 1254.
34. L.M. Robledo, R. Rodríguez-Guzmán, P. Sarriguren. Role of triaxiality in the ground-state shape of neutron-rich Yb, Hf, W, Os and Pt isotopes. J. Phys. G: Nucl. Part. Phys. 36 (2009) 115104.
35. K. Nomura et al. Derivation of IBM Hamiltonian for deformed nuclei. J. Phys.: Conf. Ser. 267 (2011) 012050.
36. I. Bentley, S. Frauendorf. Microscopic calculation of interacting boson model parameters by potential-energy surface mapping. Phys. Rev. C 83 (2011) 064322.
37. K. Nomura et al. Microscopic formulation of the interacting boson model for rotational nuclei. Phys. Rev. C 83 (2011) 041302(R).

Фахмі Ш. Радхі[1], Худа Х. Кассім[2], Муштак А. Аль-Джубборі[3], І. Хоссейн[4], Фадхіл І. Шаррад[2,5], Н. Алдахан[5], Хева І. Абдулла[6]

[1] *Факультет фізики, Коледж точних наук, Університет Басри, Басра, Ірак*
[2] *Факультет фізики, Коледж науки, Університет Кербели, Кербела, Ірак*
[3] *Факультет фізики, Коледж точних наук, Університет Мосула, Мосул, Ірак*
[4] *Факультет фізики, Коледж науки та мистецтв Рабіг, Університет короля Абдул-Азіза, Рабіг, Саудівська Аравія*
[5] *Коледж охорони здоров'я та медичних технологій, Університет Алкафіль, Наджаф, Ірак*
[6] *Кафедра фізики, Педагогічний факультет, Міжнародний університет Тішк, Ербіль, Ірак*

*Відповідальний автор: mihossain@kau.edu.sa

ОПИС ЕНЕРГЕТИЧНИХ РІВНІВ ТА ВЛАСТИВОСТЕЙ РОЗПАДУ ЯДРА ^{158}Gd

Для опису ядра ^{158}Gd використовуються моделі IBM-1 і IBM-2 із SU(3). Зроблено розрахунки енергетичних рівнів для основного стану, бета- та гамма-зон, які налічують 15 енергетичних рівнів. Однак ми виявили, що енергетичні стани з однаковим спіном у бета- та коливальних зонах стають виродженими. При порушенні динамічної симетрії SU(3) введенням парної взаємодії виродження знімається, а рівні енергії мають той же порядок, що й експериментальні.

Ключові слова: IBM-1, IBM-2, енергетичний рівень, потенційна енергія, ^{158}Gd.

Надійшла/Received 03.12.2022